Mixing of secondary organic aerosols versus relative humidity

Qing Ye[a], Ellis Shipley Robinson[a], Xiang Ding[a,b], Penglin Ye[a], Ryan C. Sullivan[a], and Neil M. Donahue[a,1]

[a]Center for Atmospheric Particle Studies, Carnegie Mellon University, Pittsburgh, PA 15213; and [b]State Key Laboratory of Organic Geochemistry, Guangzhou Institute of Geochemistry, Chinese Academy of Sciences, Guangzhou 510640, China

Edited by Barbara J. Finlayson-Pitts, University of California, Irvine, CA, and approved September 27, 2016 (received for review March 18, 2016)

Atmospheric aerosols exert a substantial influence on climate, ecosystems, visibility, and human health. Although secondary organic aerosols (SOA) dominate fine-particle mass, they comprise myriad compounds with uncertain sources, chemistry, and interactions. SOA formation involves absorption of vapors into particles, either because gas-phase chemistry produces low-volatility or semivolatile products that partition into particles or because more-volatile organics enter particles and react to form lower-volatility products. Thus, SOA formation involves both production of low-volatility compounds and their diffusion into particles. Most chemical transport models assume a single well-mixed phase of condensing organics and an instantaneous equilibrium between bulk gas and particle phases; however, direct observations constraining diffusion of semivolatile organics into particles containing SOA are scarce. Here we perform unique mixing experiments between SOA populations including semivolatile constituents using quantitative, single-particle mass spectrometry to probe any mass-transfer limitations in particles containing SOA. We show that, for several hours, particles containing SOA from toluene oxidation resist exchange of semivolatile constituents at low relative humidity (RH) but start to lose that resistance above 20% RH. Above 40% RH, the exchange of material remains constant up to 90% RH. We also show that dry particles containing SOA from α-pinene ozonolysis do not appear to resist exchange of semivolatile compounds. Our interpretation is that in-particle diffusion is not rate-limiting to mass transfer in these systems above 40% RH. To the extent that these systems are representative of ambient SOA, we conclude that diffusion limitations are likely not common under typical ambient boundary layer conditions.

secondary organic aerosols | mixing | relative humidity | single-particle mass spectrometry

Different types of organic aerosols can phase-separate, most notably nonpolar primary organic aerosol (POA) and relatively polar secondary organic aerosols (SOA). Asa-Awuku et al. (1) reported limited miscibility between motor oil POA and SOA derived from β-caryophyllene, and Robinson et al. (2) showed that particles of squalane POA and SOA derived from toluene photooxidation persisted as an external mixture for more than 3 h after being combined into a single well-mixed Teflon chamber. Theory supports high activity coefficients for these dissimilar mixtures (3), yet detailed calculations of phase partitioning thermodynamics suggest that, at least within a single more or less similar type (e.g., α-pinene SOA), the constituents are well mixed over a broad relative humidity (RH) range (4).

Even if thermodynamics favors a single, relatively ideal organic phase, diffusive limitations within particles may impede mixing driven by absorption and heterogeneous chemistry. So-called "glassy" organic aerosols associated with highly viscous states were first considered in the context of water uptake into particles at low temperature in the free troposphere (5). Much of the research into viscous organic particles has been based on rheological properties, specifically, direct measurements of their viscosity or their tendency to bounce. Virtanen et al. (6) reported that SOA formed from biogenic precursors adopt an amorphous solid state based on particle bounce in an aerosol impactor. Power et al. (7) measured viscosity of aerosol particles according to their relaxation time after being induced to coalesce. Renbaum-Wolff et al. (8) and Song et al. (9) examined supermicron SOA samples using the mobility of embedded tags and poke-flow measurements to determine the viscosity of SOA formed from α-pinene and toluene over a wide humidity range. However, highly viscous states can span orders of magnitude in terms of diffusivity in the condensed phase (10), and thus the mere presence of a viscous or semisolid state provides limited information on diffusivity, the property that control the timescales for uptake of semivolatile organic vapors into particles.

Some more direct measurements of mass transfer among particles containing SOA have been reported. Abramson et al. (11) derived chemical diffusion by trapping large hydrophobic molecules inside particles containing SOA. Perraud et al. (12) reported that, under extremely dry conditions, the adsorbed organic nitrates became buried in SOA particles. However, they did not rule out the possibility that the "trapped" species reacted with the SOA and thus remained in the condensed phase. Bones et al. (13) and Price et al. (14), using optical tweezers, explored the limitation of water transport in aerosols containing organic materials. Li et al. (15) inferred liquid to nonliquid state transition of particles containing SOA by looking at ammonia reactive uptake. However, water and ammonia are very different from semivolatile organic vapors (SVOC) produced during SOA formation in terms of molecular size and reactivity, and thus, presumably, diffusivity.

Evaporation is another potential probe of diffusion limitations. For instance, Vaden et al. (16) found that SOA evaporation is slower than predicted by a dynamical model, and also that coatings inhibit evaporation, and concluded that particles containing SOA do not exist in a liquid state. However, Saleh et al.

Significance

Recent studies called into question whether diffusion in "glassy" atmospheric secondary organic aerosols (SOA) is fast enough for phase partitioning to equilibrate, as commonly assumed in models; however, most of those studies relied on rheological measurements or uptake of small molecules such as water and ammonia. Here, we conduct unique SOA mixing experiments using single-particle mass spectrometry to probe the diffusion of semivolatile organics into SOA derived from toluene and α-pinene at different relative humidities. Results show that, if the SOA systems are representative, equilibrium partitioning likely does have time to occur in the boundary layer. This work directly probes uptake of semivolatile organics by SOA particles over a wide humidity range.

Author contributions: Q.Y. and N.M.D. designed research; Q.Y. and X.D. performed research; E.S.R. contributed new reagents/analytic tools; Q.Y., X.D., and P.Y. analyzed data; and Q.Y., R.C.S., and N.M.D. wrote the paper.

The authors declare no conflict of interest.

This article is a PNAS Direct Submission.

[1]To whom correspondence should be addressed. Email: nmd@andrew.cmu.edu.

This article contains supporting information online at www.pnas.org/lookup/suppl/doi:10.1073/pnas.1604536113/-/DCSupplemental.

(17) used a sudden temperature jump to induce a small diameter change in particles containing SOA derived from α-pinene and reported that particles reequilibrated with a timescale less than tens of minutes, which indicated an effective mass accommodation coefficient $\alpha > 0.1$. This finding highlights a challenge. At least three interconnected factors can influence evaporation behavior: diffusion limitations within particles, mass accommodation at the particle surface, and the volatility itself. Furthermore, interactions among these factors have important implications for the dynamics of SOA particle populations (18, 19).

Although glassiness can inhibit water uptake into particles, water can also soften particles containing SOA by lowering the glass transition temperature of the mixture (20). Studies have shown that increased humidity can change particles containing SOA from highly viscous semisolids to liquids (8, 18), with derived diffusion constants increasing by more than eight orders of magnitude. However, the extent to which low diffusivity in particles containing SOA actually inhibits vapor absorption—the ability of particles to take up vapors when they are exposed to semivolatile compounds—remains underexplored and highly uncertain.

Our first goal is to test whether diffusivity of SVOC in some particles containing SOA can be low enough to inhibit semivolatile organic vapor absorption into the particles, but also whether water (humidity) can increase that diffusivity by plasticizing highly viscous particles. Our second goal is to determine the relative humidity where any diffusion barrier subsides. Our third goal is to measure the fraction of common SOA types that is functionally semivolatile, meaning that vapors can exchange between different particles in several hours or less at atmospherically relevant concentrations. We use the timescale and extent of vapor exchange to infer diffusivity, observed by the change in chemical composition of distinct particle compositions brought into the same volume, which we refer to as "contact" in the figures. Using experiments employing isotopically labeled external mixtures described by Robinson et al. (21), we focus on the vapor sorption behavior of particles containing SOA generated by photooxidation of toluene and ozonolysis of α-pinene, which are commonly used as representative precursors for anthropogenic and biogenic SOA, respectively. Single-particle mass spectral measurements allow us to distinguish the aerosol sample after two populations have been brought together in the same chamber and to quantitatively assess the degree of semivolatile exchange between those populations. This exchange is the fundamental process governing the approach to equilibrium in aerosol populations (22), so these experiments directly measure that equilibration.

Results

We performed experiments probing the vapor exchange of SOA (O:C ≈ 0.6, modal mobility diameter between 300 nm and 600 nm) derived from oxidation of H_8 toluene (H-toluene SOA) and D_8 toluene (D-toluene SOA) at various RH and 22° C. We prepared one toluene SOA population in a 10 m^3 chamber (the "chamber" population) and another in a 100-L sampling bag (the "probe" population), illustrated in Fig. S1. We subsequently combined the two populations in the chamber and explored their mixing behavior using a light-scattering single-particle aerosol mass spectrometer (LSSP-AMS; Aerodyne Inc.) (23). After combination, the chamber particle population had a suspended mass concentration of ∼100 $\mu g \cdot m^{-3}$, and the probe population had a mass concentration of ∼40 $\mu g \cdot m^{-3}$. We collected single-particle data at unit mass resolution and will discuss signals at a given mass to charge ratio, where s_x is the raw signal at $m/z = x$. Fig. 1 shows results from the single-particle mode, and Fig. S2 shows time sequence data from bulk measurements.

Toluene SOA Mixing in a Dry Chamber. We first present an experiment conducted under continuously dry conditions (the chamber RH remained less than 7% throughout the experiment). We show time sequences from AMS bulk measurements of H-toluene SOA, D-toluene SOA, and their unique fragment signals (s_{43}, mostly $C_2H_3O^+$, and s_{46}, mostly $C_2D_3O^+$) in Fig. S2*A* and the SOA mass spectra in Fig. S3. We produced the H-toluene SOA in the main chamber, and, at time = 0, we transferred D-toluene SOA produced in the sampling bag (the probe population) into the main chamber.

In Fig. 1*A*, we show the analysis of each particle in this dry experiment. For the 2.5 h following combination of the two populations into the same experimental volume, most of the particles have deuterium content near unity or zero, meaning the large majority of particles remain either mostly deuterated or mostly hydrogenated. As we describe in *Materials and Methods*, the approximate deuterium content is $f_D = s_{46}/(s_{43} + s_{46})$. Using f_D as a numerical filter, we separate the individual particle mass spectra into two groups: particles that were originally pure H-toluene SOA and particles that were originally pure D-toluene SOA. We then add the spectra in 30-min bins, which gives sufficient signal for quantitative analysis. After this step, we calculate the mass percentage of the probe material (in this case, the D-toluene SOA) in both the chamber and probe populations, which we plot with connected, closed circles in Fig. 1. These aggregated values inform our quantitative assessment (*SI Materials and Methods*).

During the dry experiment, we transferred the D-toluene SOA probe particles (a minor constituent) into the main chamber containing H-toluene SOA (particles and vapors). Those probe particles sorbed some vapors from the H-toluene SOA, stabilizing at less than 10% H content immediately after being injected into the main chamber. The H-toluene SOA chamber particles remained completely devoid of D-toluene SOA throughout the experiment. Note that, if the small amount of mixing were due to coagulation, we would expect to observe the reverse effect, where relatively high concentrations of the newly introduced D-toluene SOA probe particles could potentially strike some (already highly dilute) H-toluene SOA particles; there is no sign of this, and thus we conclude that a small fraction of H-toluene SOA vapors absorbed or adsorbed onto the D-toluene particles. However, after this small initial uptake, there was no further exchange of vapors between the two populations; they remained chemically distinct from each other with essentially constant composition thereafter.

Because we generated the two SOA populations from identical precursors (except that one is isotopically labeled), they should be completely miscible thermodynamically. Thus, the evident lack of mixing could have two causes: high viscosity (low diffusivity) in the particles or simply a dearth of semivolatile vapors available for exchange. Robinson et al. (21) previously showed, in a procedurally identical mixing experiment of SOA derived from toluene and α-pinene (with α-pinene SOA as the probe population), that vapors from toluene SOA substantially infiltrated α-pinene SOA particles (Fig. S4), with those particles reaching a 35% toluene SOA mass fraction promptly after entering the main chamber at RH less than 5% (21). This indicates that the toluene SOA aerosol produced in the main chamber included semivolatile vapors that would have sorbed into the probe particles if possible. The 10% sorption of semivolatiles to the probe particles in the dry chamber may have been surface adsorption or may reveal limited diffusion into a thin disrupted surface layer. However, at least 3 times more material can sorb into the probe particles at higher RH. Therefore, the lack of mixing is likely due to low diffusivity in particles comprised of toluene SOA.

Toluene SOA Mixing in Damp, Moist, and Wet Chambers. Next we present experiments conducted at elevated RH. We performed exactly the same mixing experiments described in *Toluene SOA Mixing in a Dry Chamber*, but, shortly after bringing the two SOA populations into contact, we raised the chamber RH to different

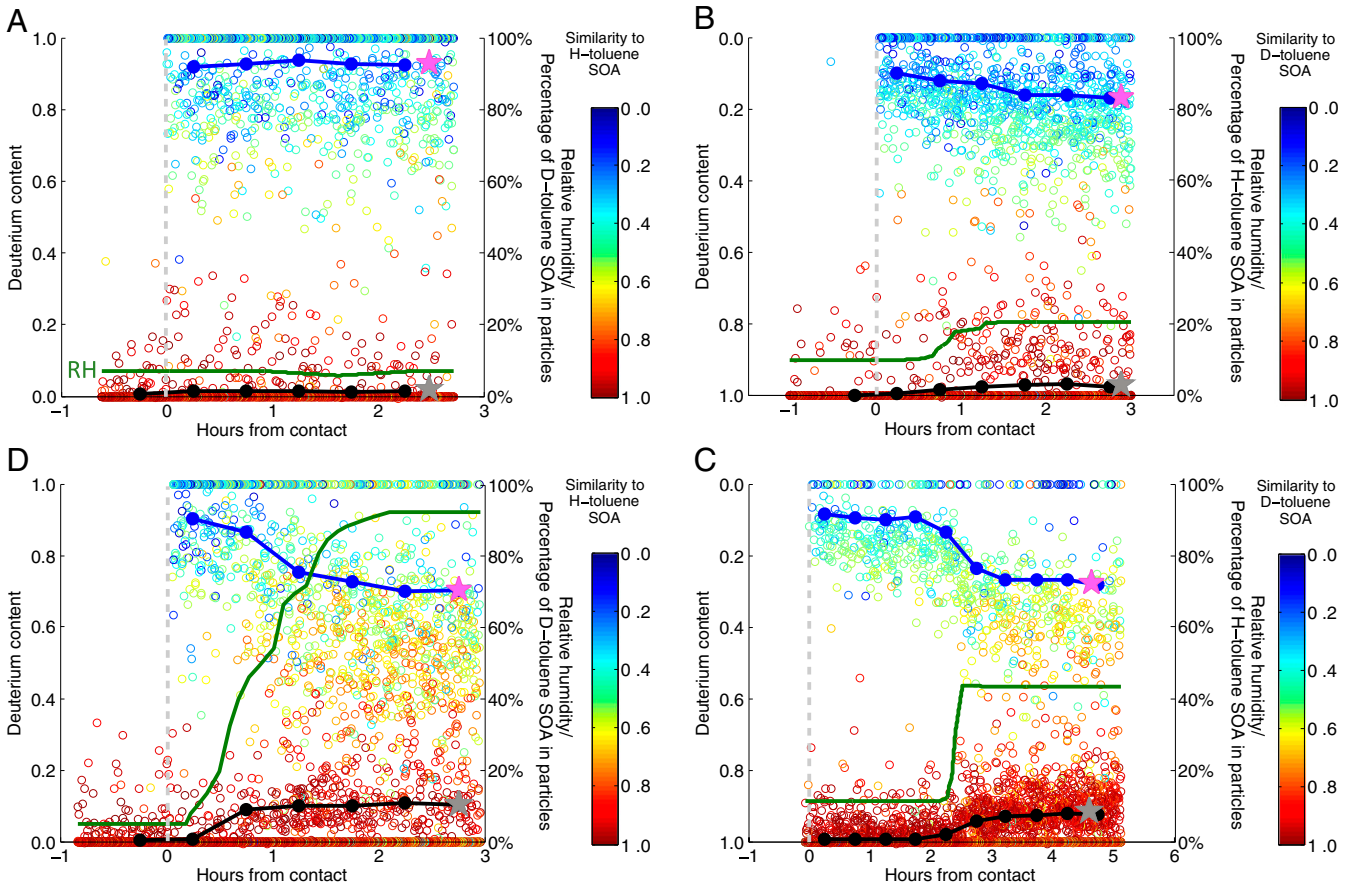

Fig. 1. Light-scattering single-particle data for mixing experiments of SOA formed from H-toluene SOA and D toluene with various RH profiles. The green curves show RH. At $t = 0$ h, we introduced SOA particles produced in a secondary bag (the probe population) into the main chamber prefilled with another SOA population (the chamber population). Each symbol corresponds to a single particle, plotted according to the approximate deuterium content. The symbol color indicates the similarity to the chamber SOA population in each experiment. There is no evidence that particle composition varies significantly within a population; instead, the small-number statistics make individual particle signals noisy (including 0 and 100% signals). We thus aggregate signals every 30 min to derive the probe SOA content in each particle population (*y* axis on the right; H-toluene SOA for *B* and *C*, and D-toluene SOA for *A* and *D*), shown with connected symbols. The pink and gray stars represent the percentage of probe SOA content in each particle population 2.5 h after water injection. (*A*) Dry chamber (7% RH). Particles remained mostly purely deuterated or hydrogenated with no significant mass exchange through the entire experiment. (*B*) Damp chamber (20% RH added after particle contact). Slow mixing into probe particles and some mixing into chamber particles is evident. (*C*) Moist chamber (43% RH). Rapid mixing up to a mass fraction of 0.3 in the probe particles. (*D*) Wet chamber (90% RH). Identical mixing to *C* well before maximum RH.

levels by adding water vapor to the chamber. We show the bulk data in *Supporting Information*. In Fig. 1 *B–D*, we show single-particle data from experiments in a damp chamber with 20% RH, a moist chamber with 43% RH, and a wet chamber with up to 90% RH, respectively. Similar to the dry-chamber case, in the wet-chamber experiment, we used D-toluene SOA particles as the probe population; however, in the damp-chamber and moist-chamber cases, we used H-toluene SOA as the probe particles so that we obtained "blank" spectra at $t < 0$ h for both SOA populations.

In Fig. 1*B*, we see the onset of slow vapor exchange in the damp chamber. The probe population started to progressively absorb vapor from the chamber population at 20% RH, indicating that even a modest amount of water can sufficiently soften particles comprising toluene SOA to reduce diffusion limitations within them. At 43% RH, the probe population (H-toluene SOA) reached roughly 30% chamber SOA content (D-toluene SOA) in about 0.5 h. The chamber population, which remained completely pure in the dry experiment, took up 10% of the probe material. From the data in Fig. 1*D*, we see similar mixing at 43% and 90% RH. A large fraction of the D-toluene probe particles gained a significant fraction from H-toluene SOA, reaching roughly 30% H-toluene SOA content after 3 h, and, concurrently, the chamber particles absorbed ∼10% probe SOA content.

In Fig. 2, we show the extent of mixing in the two populations 2.5 h after water injection as a function of RH. The pink and gray stars correspond to the stars in Fig. 1. This graph shows that mixing after 2.5 h becomes facile between 20% and 40% RH, reaching asymptotic values above 40% RH.

Toluene SOA Mixing with α-Pinene SOA. When Robinson et al. (21) added α-pinene SOA to a chamber containing D-toluene SOA at low RH, the α-pinene SOA probe particles took up a significant fraction of D-toluene SOA; however the D-toluene SOA particles showed no evidence of α-pinene products (Fig. S4). The rapid absorption of toluene SOA into the α-pinene SOA probe particles indicates two things. First, even at low RH, the toluene SOA system contains a substantial semivolatile fraction (and thus the reversal of accretion products after condensation is not the principal cause of the RH dependence we observe in the toluene SOA system). Second, unlike the toluene-derived SOA, the α-pinene-derived SOA does not have a diffusive limitation to uptake of semivolatile organics, even under dry conditions. However, the question remains whether the α-pinene SOA simply did not

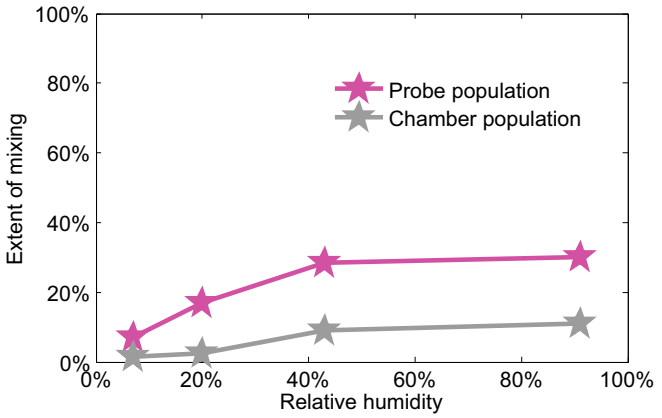

Fig. 2. The extent of mixing for toluene-derived SOA vs. RH, 2.5 h after water vapor injection. Extent of mixing is the mass fraction of isotopically labeled probe material in chamber particles. The pink and gray stars correspond to the stars in Fig. 1. Vapor exchange begins to occur (in 2.5 h) at 20% RH. Above 40% RH, mixing after 2.5 h stabilizes at about 30% for the probe population and 10% for the chamber population; this is consistent with the mass fractions of these two populations in the chamber.

contain a significant fraction of semivolatile condensable vapors, or whether diffusion into the toluene SOA was simply slow at low RH. Therefore, we repeated the mixing experiment between α-pinene SOA and toluene SOA (21), but we added water vapor to the chamber.

In Fig. 3, we show the RH effect for this system. As with the toluene SOA system, when RH increased, the toluene SOA particles in the chamber absorbed a substantial fraction of semivolatile vapors, this time from α-pinene SOA. Thus, the lack of absorption of α-pinene SOA into toluene SOA particles reported by Robinson et al. (21) was evidently due to low diffusivity at low RH. Fig. 3 shows that the fraction of toluene SOA in the α-pinene SOA particles reached a steady state of 20 to 30% under the same conditions as the experiments with isotopically labeled toluene SOA; this is slightly reduced uptake compared with the pure toluene SOA isotopic exchange. It may be that the α-pinene and toluene SOA systems form a slightly nonideal solution, or this difference may be due to experimental variability. However, this finding is broadly consistent with toluene-SOA and α-pinene SOA forming a nearly ideal solution, in agreement with Hildebrandt et al. (24).

Robinson et al. (21) observed a somewhat higher uptake of toluene SOA vapor into particles containing α-pinene SOA (Fig. S3), but the overall mass loading of SOA was also roughly 3 times higher in those experiments than in ours. As shown by Ye et al. (25), the "semivolatile" fraction of SOA measured with probe particles (in that case, polyethylene glycol) increases as more precursor is oxidized and the activity of the semivolatile species consequently rises. Regardless, the influence of RH on vapor uptake by particles consisting of toluene-derived SOA is obvious in Fig. 3.

Discussion

Presuming that these systems are completely miscible, the compositions of all particles should converge to a single internal mixture. However, our observations clearly show that the populations do not completely mix over hours, even when RH is >90%. This lack of complete mixing could have one of two causes: diffusion limitations within (glassy, viscous) particles or a fraction of the SOA with very low volatility that thus does not have time to move from one population to the other.

Low measured viscosity of toluene SOA particles at 90% RH almost certainly corresponds to high diffusivity, allowing complete mixing within a fraction of a second (8, 10) Furthermore, the volatility distribution of toluene-derived SOA spans a very wide range (26, 27). We thus conclude that the 30% mixing at elevated RH is due to a preponderance of low-volatility material in the toluene SOA (70% by mass) that does not have time to exchange during these experiments. We observe the same extent of mixing between 40% and 90% RH, where viscosity changes by five orders of magnitude (9), and so we conclude that in-particle diffusion for 300- to 600-nm toluene SOA particles is likely not rate limiting for mass exchange above 40% RH. However, the suppressed mixing evident in Fig. 2 at lower RH is consistent with decreased diffusivity within the drier, more viscid particles limiting mass transfer to the bulk of the individual particles at low RH.

Semivolatile organics can partition onto Teflon chamber walls, which can lead to an underestimation of SOA yields (28, 29). Loss of semivolatile organics in our smaller 100-L bag could be especially significant. If some vapors were denuded from the probe aerosol population by the high surface-area-to-volume ratio of the 100-L preparation bag, this would limit semivolatile vapors from the probe aerosol. However, our results at elevated RH show that our probe aerosol population did contain a significant semivolatile fraction, because semivolatile probe material transferred, to a significant extent, into the chamber particles. Furthermore, to the extent that the 100-L sample preparation bag denuded some of the semivolatile constituents from the probe aerosol population, it is likely that this rendered the particles more glassy; the residual material must have been less volatile, and thus some combination of higher molecular weight and more polar, both of which increase the glass transition temperature (20). Even in the presence of potentially absorptive Teflon walls, our results confirm that a significant fraction (30% or more) of the SOA constituents are semivolatile and can move from one particle population to another for several hours in our chamber.

The mixing we observe at elevated RH is consistent with the findings of Renbaum-Wolff et al. (8), who found that, at elevated RH, the viscosity of α-pinene SOA decreased by orders of magnitude. Furthermore, Bateman et al. (30) observed a transition from bouncy to sticky behavior of both α-pinene and toluene SOA at elevated RH, consistent with a state change from a semisolid to liquid phase. We observe the onset of mixing at 20% RH for toluene SOA. The mixing appears to be unimpeded above 43% RH, much lower than the 70% RH viscosity threshold (8, 30). Particles can appear to be solid or semisolid and still have relatively rapid diffusion of semivolatile organics (7).

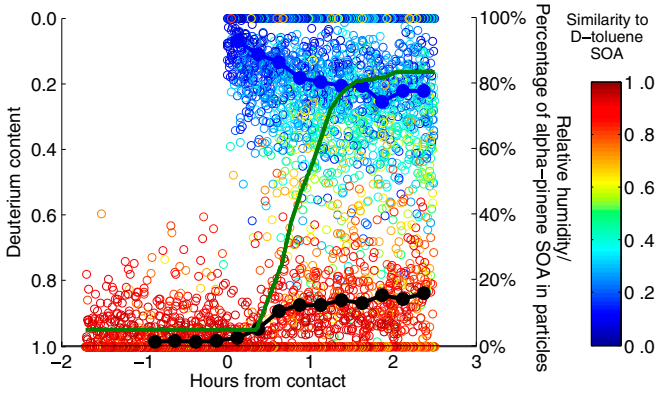

Fig. 3. Light-scattering single-particle data for mixing of α-pinene SOA and D-toluene SOA at elevated RH. As with the isotopically labeled toluene SOA experiment, at high RH, a substantial amount of vapors are exchanged, so the similarity scores of the two populations converge. By the end of the experiment, the α-pinene SOA particles contain 20 to 30% D-toluene SOA.

We also observe a pronounced difference between toluene-derived SOA and α-pinene-derived SOA at low RH, consistent with the high viscosity reported by Song et al. (9). At elevated RH, in addition to plasticizing particles containing SOA, water could also induce chemistry or change the activity coefficients of semivolatile compounds. However, our results suggest that the latter two effects play a minor role, because we observed very similar extent of mixing at 43% and 90% RH (Fig. 2). Furthermore, in the mixing experiment between SOA from α-pinene and from toluene under dry conditions, the α-pinene SOA takes up a substantial fraction of vapors from toluene SOA. This indicates that diffusion plays the leading role limiting SVOC uptake into toluene-derived particles at low RH in our experiments. In addition, a complementary study on similar systems measuring evaporation rates from an oscillating microbalance also shows that evaporation rates from toluene SOA are suppressed at low RH but remain constant for α-pinene SOA, which is consistent with our findings and inter-pretation (31).

Uptake of small molecules is also related to diffusivity. Price et al. (14) observed diffusion of D_2O into α-pinene-derived SOA discs over a wide range of water activities and temperatures. They observed low diffusivity of water only at very low temperature and water activity; their warmest samples at 7 °C showed a minimum diffusivity of 10^{-13} $m^2 \cdot s^{-1}$ at a water activity of 0.1, corresponding to equilibration of order 1 s. Li et al. (15) observed a relatively sharp transition in NH_3 reactive uptake into toluene-derived SOA between 20% and 40% RH. They also observed a more gradual increase in NH_3 uptake into α-pinene-derived SOA between dry conditions and 40% RH. Both experiments suggest that diffusion limitations vanish above roughly 40% RH, and both suggest that diffusion is somewhat slower in toluene-derived SOA than in α-pinene-derived SOA when diffusion limitations exist. However, the mixing experiments show little evidence for mixing limitations in α-pinene-derived SOA under any conditions, whereas the ammonia uptake is sensitive to RH below 30% RH. Just as with rheological properties, reactive uptake is also not the same as phase equilibration, and small molecules may behave very differently from larger semivolatile organic compounds. If anything, we would expect diffusion to be more difficult for the larger semivolatile species. However, in α-pinene-derived SOA, we see no signs of diffusive limitations even under dry conditions, whereas reactive uptake of NH_3 is suppressed.

The extent of mixing at high RH also constrains the volatility distribution of the SOA. As shown in Donahue et al. (32), the timescale for evaporation of $C^* = 10$ $\mu g \cdot m^{-3}$ compounds from 500-nm particles is roughly 1 h, so these isotopic mixing experiments constrain the fraction of this SOA with $C^* \geq 10$ $\mu g \cdot m^{-3}$, provided that diffusion within the particles is faster than 1 h. Compounds with $C^* \lesssim 1$ $\mu g \cdot m^{-3}$ would not exchange in $\lesssim 10$ h under any circumstances. Taken together, these experiments indicate that roughly 30% of toluene SOA is effectively semivolatile, with $C^* \geq 10$ $\mu g \cdot m^{-3}$ when the total SOA loading is roughly 30 $\mu g \cdot m^{-3}$. This finding indicates an effective semivolatile activity of 0.30 in both phases (the activity is the fraction in the particles and the saturation ratio in the gas phase). If the semivolatile material consisted of a single product with $C^* = 30$ $\mu g \cdot m^{-3}$, that would imply a particle concentration of 9 $\mu g \cdot m^{-3}$, a vapor concentration of 9 $\mu g \cdot m^{-3}$ (thus the 0.30 activity in each phase), and an equilibrium partitioning fraction of 0.5, consistent with equilibrium partitioning theory when $C^* = C_{OA}$ (33). Our data also suggest that the remaining 70% of the toluene SOA had a sufficiently low volatility to show limited exchange in several hours. Based on the characteristic evaporation timescales (32), this fraction has a volatility $C^* \leq 1$ $\mu g \cdot m^{-3}$.

In most of the atmospheric boundary layer worldwide, the relative humidity is usually higher than our damp chamber (20% RH) (34, 35), where diffusion limitations in particles comprising toluene-derived SOA start to subside. We observe exchange of semivolatile vapors into submicron particles comprising toluene-derived SOA in 30 mins or less for RH of 40% or above. This mixing timescale is, in most circumstances, shorter than the timescale for significant meteorological and chemical changes in the atmosphere. Therefore, diffusion limitations within particles comprising SOA species comparable to those we have studied here should not significantly hinder equilibration of semivolatile organic compounds. Furthermore, this timescale is also similar to or shorter than the time step used in many chemical transport models, in which gas–particle phase equilibration is assumed (36, 37). The systems we investigated—α-pinene SOA and toluene SOA—are widely used as SOA surrogates for the monoterpene family from biogenic sources and the alkyl-aromatics family from anthropogenic sources in chemical transport models (36, 38–40). These are major SOA sources. However, diffusion and mixing within SOA particles formed from intermediate volatile organic compounds (IVOC) remains to be tested; as with sesquiterpenes, IVOCs are higher molecular weight precursors that may be important sources of SOA (41, 42), and so there remains the possibility that these species, or mixtures of them, may produce particles with lower diffusivity than those we have studied here.

Conclusions

The experiments we describe here directly test the timescale for mixing of semivolatile compounds into particles containing secondary organic aerosol, over timescales (several hours) relevant to atmospheric transport and diurnal cycling. Our work demonstrates how laboratory SOA mixing experiments using single-particle mass spectrometer measurements can effectively probe the mixing behavior of particles containing SOA under realistic conditions. We have shown that SOA derived from toluene does indeed resist uptake of semivolatile vapors, but only at very low relative humidity. This in-particle diffusion is not rate-limiting to mass transfer above 40% RH in our system.

A major reason for the interest in low diffusivity within atmospheric particles is that this could slow down the equilibration of semivolatile SOA mass. Our experiments directly probe semivolatile mass exchange over the full range of atmospheric RH. We have also shown that toluene SOA contains about 30% semivolatile material ($C^* \gtrsim 10$ $\mu g \cdot m^{-3}$), whereas the remaining 70% has a volatility $C^* \lesssim 1$ $\mu g \cdot m^{-3}$. If these results extend to atmospheric organic aerosols, which are often much more oxidized than the laboratory-generated SOA particles in this study (43), then diffusion limitations are unlikely to prevent relatively rapid equilibration of semivolatile organics in the planetary boundary layer on timescales above an hour or so.

Materials and Methods

We describe the methods in detail in *Supporting Information*. In brief, we followed the methods of Robinson et al. (21) to prepare SOA populations in separate smog chambers and then combined the populations into one chamber. We used single-particle aerosol mass spectrometry (23) to group the particles based on their original content, aggregated individual particle signals to obtain sufficient signal-to-noise, and analyzed these aggregated spectra to determine the fractions of each original SOA type in the two populations.

ACKNOWLEDGMENTS. This work was supported by the Wallace Research Foundation, National Science Foundation Grants 0922643 and 1412309, the US Environmental Protection Agency Science to Achieve Results program, and the Faculty for the Future Fellowship from Schlumberger Foundation.

1. Asa-Awuku A, Miracolo M, Kroll J, Robinson A, Donahue N (2009) Mixing and phase partitioning of primary and secondary organic aerosols. *Geophys Res Lett* 36(15): L15827.
2. Robinson ES, Saleh R, Donahue NM (2015) Probing the evaporation dynamics of mixed SOA/squalane particles using size-resolved composition and single-particle measurements. *Environ Sci Technol* 49(16):9724–9732.
3. Donahue NM, Epstein S, Pandis SN, Robinson AL (2011) A two-dimensional volatility basis set: 1. Organic-aerosol mixing thermodynamics. *Atmos Chem Phys* 11(7): 3303–3318.
4. Zuend A, Seinfeld J (2012) Modeling the gas-particle partitioning of secondary organic aerosol: The importance of liquid-liquid phase separation. *Atmos Chem Phys* 12(9):3857–3882.
5. Zobrist B, Marcolli C, Pedernera D, Koop T (2008) Do atmospheric aerosols form glasses? *Atmos Chem Phys* 8(17):5221–5244.
6. Virtanen A, et al. (2010) An amorphous solid state of biogenic secondary organic aerosol particles. *Nature* 467(7317):824–827.
7. Power R, Simpson S, Reid J, Hudson A (2013) The transition from liquid to solid-like behaviour in ultrahigh viscosity aerosol particles. *Chem Sci (Camb)* 4(6):2597–2604.
8. Renbaum-Wolff L, et al. (2013) Viscosity of α-pinene secondary organic material and implications for particle growth and reactivity. *Proc Natl Acad Sci USA* 110(20): 8014–8019.
9. Song M, et al. (2016) Relative humidity-dependent viscosity of secondary organic material from toluene photo-oxidation and possible. *Atmos Chem Phys* 16(14): 8817–8830.
10. Shiraiwa M, Ammann M, Koop T, Pöschl U (2011) Gas uptake and chemical aging of semisolid organic aerosol particles. *Proc Natl Acad Sci USA* 108(27):11003–11008.
11. Abramson E, Imre D, Beránek J, Wilson J, Zelenyuk A (2013) Experimental determination of chemical diffusion within secondary organic aerosol particles. *Phys Chem Chem Phys* 15(8):2983–2991.
12. Perraud V, et al. (2012) Nonequilibrium atmospheric secondary organic aerosol formation and growth. *Proc Natl Acad Sci USA* 109(8):2836–2841.
13. Bones DL, Reid JP, Lienhard DM, Krieger UK (2012) Comparing the mechanism of water condensation and evaporation in glassy aerosol. *Proc Natl Acad Sci USA* 109(29):11613–11618.
14. Price HC, et al. (2015) Water diffusion in atmospherically relevant α-pinene secondary organic material. *Chem Sci (Camb)* 6(8):4876–4883.
15. Li YJ, et al. (2015) Chemical reactivity and liquid/nonliquid states of secondary organic material. *Environ Sci Technol* 49(22):13264–13274.
16. Vaden TD, Imre D, Beránek J, Shrivastava M, Zelenyuk A (2011) Evaporation kinetics and phase of laboratory and ambient secondary organic aerosol. *Proc Natl Acad Sci USA* 108(6):2190–2195.
17. Saleh R, Donahue NM, Robinson AL (2013) Time scales for gas-particle partitioning equilibration of secondary organic aerosol formed from alpha-pinene ozonolysis. *Environ Sci Technol* 47(11):5588–5594.
18. Shiraiwa M, Zuend A, Bertram AK, Seinfeld JH (2013) Gas-particle partitioning of atmospheric aerosols: Interplay of physical state, non-ideal mixing and morphology. *Phys Chem Chem Phys* 15(27):11441–11453.
19. Shiraiwa M, et al. (2013) Size distribution dynamics reveal particle-phase chemistry in organic aerosol formation. *Proc Natl Acad Sci USA* 110(29):11746–11750.
20. Koop T, Bookhold J, Shiraiwa M, Pöschl U (2011) Glass transition and phase state of organic compounds: Dependency on molecular properties and implications for secondary organic aerosols in the atmosphere. *Phys Chem Chem Phys* 13(43): 19238–19255.
21. Robinson ES, Saleh R, Donahue NM (2013) Organic aerosol mixing observed by single-particle mass spectrometry. *J Phys Chem A* 117(51):13935–13945.
22. Marcolli C, Luo B, Peter T, Wienhold F (2004) Internal mixing of the organic aerosol by gas phase diffusion of semivolatile organic compounds. *Atmos Chem Phys* 4(11-12): 2593–2599.
23. Cross ES, et al. (2007) Laboratory and ambient particle density determinations using light scattering in conjunction with aerosol mass spectrometry. *Aerosol Sci Technol* 41(4):343–359.
24. Hildebrandt L, et al. (2011) Evaluating the mixing of organic aerosol components using high-resolution aerosol mass spectrometry. *Environ Sci Technol* 45(15): 6329–6335.
25. Ye P, Ding X, Ye Q, Robinson ES, Donahue NM (2016) Uptake of semi-volatile secondary organic aerosol formed from α-pinene into non-volatile polyethylene glycol probe particles. *J Phys Chem A* 120(9):1459–1467.
26. Hildebrandt L, Donahue NM, Pandis SN (2009) High formation of secondary organic aerosol from the photo-oxidation of toluene. *Atmos Chem Phys* 9(9):2973–2986.
27. Hildebrandt Ruiz L, et al. (2015) Formation and aging of secondary organic aerosol from toluene: Changes in chemical composition, volatility, and hygroscopicity. *Atmos Chem Phys* 15(14):8301–8313.
28. Matsunaga A, Ziemann PJ (2010) Gas-wall partitioning of organic compounds in a teflon film chamber and potential effects on reaction product and aerosol yield measurements. *Aerosol Sci Technol* 44(10):881–892.
29. Zhang X, et al. (2014) Influence of vapor wall loss in laboratory chambers on yields of secondary organic aerosol. *Proc Natl Acad Sci USA* 111(16):5802–5807.
30. Bateman AP, Bertram AK, Martin ST (2015) Hygroscopic influence on the semisolid-to-liquid transition of secondary organic materials. *J Phys Chem A* 119(19):4386–4395.
31. Liu P, et al. Lability of secondary organic particulate matter. *Proc Natl Acad Sci USA* 113(45):12643–12648.
32. Donahue NM, Robinson AL, Trump ER, Riipinen I, Kroll JH (2014) Volatility and aging of atmospheric organic aerosol. *Top Curr Chem* 339:97–143.
33. Donahue NM, Robinson AL, Stanier CO, Pandis SN (2006) Coupled partitioning, dilution, and chemical aging of semivolatile organics. *Environ Sci Technol* 40(8): 2635–2643.
34. Wallace JM, Hobbs PV (2006) *Atmospheric Science: An Introductory Survey* (Academic, San Diego), Vol 92.
35. Garratt JR (1994) Review: The atmospheric boundary layer. *Earth Sci Rev* 37(1-2): 89–134.
36. Shrivastava M, et al. (2015) Global transformation and fate of SOA: Implications of low-volatility SOA and gas-phase fragmentation reactions. *J Geophys Res* 120(9): 4169–4195.
37. Chung SH, Seinfeld JH (2002) Global distribution and climate forcing of carbonaceous aerosols. *J Geophys Res* 107(D19):4407.
38. Carlton AG, et al. (2010) Model representation of secondary organic aerosol in CMAQv4.7. *Environ Sci Technol* 44(22):8553–8560.
39. Pye HO, Seinfeld JH (2010) A global perspective on aerosol from low-volatility organic compounds. *Atmos Chem Phys* 10(9):4377–4401.
40. Emmons L, et al. (2010) Description and evaluation of the Model for Ozone and Related Chemical Tracers, version 4 (MOZART-4). *Geosci Model Dev* 3(1):43–67.
41. Robinson AL, et al. (2007) Rethinking organic aerosols: Semivolatile emissions and photochemical aging. *Science* 315(5816):1259–1262.
42. Zhao Y, et al. (2014) Intermediate-volatility organic compounds: A large source of secondary organic aerosol. *Environ Sci Technol* 48(23):13743–13750.
43. Jimenez JL, et al. (2009) Evolution of organic aerosols in the atmosphere. *Science* 326(5959):1525–1529.